Published in final edited form as:
Biochem Pharmacol. 2012 December 15; 84(12): 1571–1580. doi:10.1016/j.bcp.2012.09.005.

Apigenin induces DNA damage through the PKCδ-dependent activation of ATM and H2AX causing down-regulation of genes involved in cell cycle control and DNA repair

Daniel Arango[a,b,d], **Arti Parihar**[a,b,c], **Frederick A. Villamena**[c,e], **Liwen Wang**[f,g], **Michael A. Freitas**[f], **Erich Grotewold**[a,h], and **Andrea I. Doseff**[a,b,c,*]

[a]Department of Molecular Genetics, The Ohio State University, Columbus, OH 43210, United States

[b]Department of Internal Medicine, Division of Pulmonary, Allergy, Critical Care and Sleep, The Ohio State University, Columbus, OH 43210, United States

[c]The Heart and Lung Research Institute, The Ohio State University, Columbus, OH 43210, United States

[d]Molecular, Cellular and Development Biology Graduate Program, The Ohio State University, Columbus, OH 43210, United States

[e]Department of Pharmacology, The Ohio State University, Columbus, OH 43210, United States

[f]Department of Molecular Immunology, Virology and Medical Genetics, The Ohio State University, Columbus, OH 43210, United States

[g]Department of Chemistry, The Ohio State University, Columbus, OH 43210, United States

[h]Center for Applied Plant Sciences, The Ohio State University, Columbus, OH 43210, United States

Abstract

Apigenin, an abundant plant flavonoid, exhibits anti-proliferative and anti-carcinogenic activities through mechanisms yet not fully defined. In the present study, we show that the treatment of leukemia cells with apigenin resulted in the induction of DNA damage preceding the activation of the apoptotic program. Apigenin-induced DNA damage was mediated by p38 and protein kinase C-delta (PKCδ), yet was independent of reactive oxygen species or caspase activity. Treatment of monocytic leukemia cells with apigenin induced the phosphorylation of the ataxia-telangiectasia mutated (ATM) kinase and histone H2AX, two key regulators of the DNA damage response, without affecting the ataxia-telangiectasia mutated and Rad-3-related (ATR) kinase. Silencing and pharmacological inhibition of PKCδ abrogated ATM and H2AX phosphorylation, whereas inhibition of p38 reduced H2AX phosphorylation independently of ATM. We established that apigenin delayed cell cycle progression at G1/S and increased the number of apoptotic cells. In

*Corresponding author at: 201 Heart and Lung Research Institute, The Ohio State University, 473 West 12th Avenue, Columbus, OH 43210, United States. Tel.: +1 614 292 9507; fax: +1 614 293 4799. doseff.1@osu.edu (A.I. Doseff)..

Conflict of interest The authors have declared no conflict of interest.

addition, genome-wide mRNA analyses showed that apigenin-induced DNA damage led to down-regulation of genes involved in cell-cycle control and DNA repair. Taken together, the present results show that the PKCδ-dependent activation of ATM and H2AX define the signaling networks responsible for the regulation of DNA damage promoting genome-wide mRNA alterations that result in cell cycle arrest, hence contributing to the anti-carcinogenic activities of this flavonoid.

Keywords

Flavonoids; Apoptosis; DNA damage; PKC delta

1. Introduction

Flavonoids are plant polyphenols serving as key dietary nutraceuticals recognized by their anti-inflammatory, anti-proliferative, anti-metastatic and anti-cancer activities [1–3]. Apigenin (4′,5,7-trihydroxyflavone) is a flavone abundantly found in parsley and celery, two common components of the Mediterranean diet, claimed to have potential health benefits in inflammatory diseases [4–8]. Recent epidemiological population-based studies in ovarian cancer patients showed that the intake of apigenin, but not of other flavonoids, was associated with decreased cancer risk [9]. Apigenin induces apoptosis in human monocytic leukemia cells with high efficacy [10], yet with variable effectiveness in several other cancer cell lines [11,12]. We showed that apigenin-induced apoptosis requires the protein kinase C-delta (PKCδ)-dependent activation of caspase-3, a key apoptotic regulator [10]. Apigenin-induced phosphorylation of the apoptotic inhibitor heat-shock protein 27 (Hsp27), by mitogen activated protein kinases (MAPK) p38 and PKCδ significantly increased the susceptibility of leukemia cells to apoptosis [13]. In addition, apigenin induced the production of reactive oxygen species (ROS) and the activation of p38, both dispensable for the execution of cell death [10,13,14]. Although several signaling pathways are triggered by apigenin [10,13,15], the precise mechanisms by which apigenin promotes its anti-carcinogenic effects remain poorly understood.

Commonly used anti-cancer agents exert their cytotoxic effects by inducing DNA-damage through diverse mechanisms [16–18]. Genotoxic DNA damage, especially in the form of double strand breaks (DSBs), results in the activation of a complex signaling network characterized by the activation of the ataxia telangiectasia mutated (ATM) and the ataxia-telangiectasia mutated and Rad-3-related (ATR) kinases, among others [19–23]. Activation of ATR and ATM lead to the phosphorylation of the histone H2AX [19], but these pathways have shown to have little redundancy [23,24]. Phosphorylation of H2AX at Ser-139 (γH2AX) is considered a hallmark of DSBs [25]. Activation of ATR, ATM and H2AX have an important role in the DNA damage response including stimulation of DNA repair, activation of cell cycle checkpoints, and eventually induction of apoptosis [26]. PKCδ activation was observed in several cell types in response to a variety of apoptotic and genotoxic stimuli [27–29] and is essential for etoposide-induced apoptosis [28], whereas the activation of the p38 pathway has been associated with stress-activated response and UV-radiation [30].

In spite of the growing significance of apigenin as an anti-cancer agent, its mechanisms of action remain elusive. In the present study, we established that apigenin induces DNA damage in a PKCδ and p38 dependent pathway, but independent of ROS production. Apigenin had no effect on ATR, but lead to the PKCδ-dependent activation of ATM and H2AX phosphorylation, while p38 affected H2AX in an ATM-independent fashion. Consistently, the activation of ATM checkpoints affected cell cycle progression and led to transcriptional down-modulation of genes involved in G1/S transition and DNA repair. Altogether these findings strongly establish a mechanism of apigenin-induced DNA damage revealing a complex signaling network responsible for the cytotoxic effects of this dietary compound.

2. Materials and methods

2.1. Chemicals, cell lines, and culture

THP-1 human monocytic leukemia cells obtained from ATCC (Manassas, VA) were cultured as described previously [10,13]. Caspase-3 inhibitor DEVD-FMK and the caspase-3 substrate DEVD-AFC were from Enzyme System Product (Livermore, CA). The p38 inhibitor SB203580 and the PKCδ inhibitor rottlerin were from Calbiochem (San Diego, CA), the ROS inhibitor EUK-134 was from Cayman Chemical (Ann Arbor, MI). DAPI (4′, 6-diamidino-2-phenylindole), DHE (dihydroethidium), DCFDA (2,7-dichlorofluorescein diacetate) and protein A agarose beads were purchased from Invitrogen (Carlsbad, CA). Apigenin, diluent dimethyl sulfoxide (DMSO), normal and low melting point agarose (NMPA and LMPA respectively) and all other chemicals were from Sigma (St. Louis, MO).

2.2. Alkaline comet assay

DNA damage was assessed by the alkaline comet assay (single cell gel electrophoresis) as described [31]. Briefly, a mix of cell suspension (20 μl; 10^6 cells/ml) and 0.6% LMPA (80 μl) were dipped onto microscope slides pre-coated with 1% NMPA and covered with coverslips at 4 °C for 5 min. Coverslips were removed and slides were covered with 0.6% LMPA and incubated at 4 °C for 5 min with coverslips. Coverslips were removed and slides were immersed overnight in lysis buffer (2.5 M NaCl, 100 mM Na_2EDTA, 10 mM Tris, 1% Na-N-lauryl sarcosinate, 10% DMSO, 1% Triton X-100, pH 10). Slides were incubated for 30 min in alkaline buffer (300 mM NaOH, 1 mM Na_2EDTA, pH 13) followed by electrophoresis at 28 V and 300 mA for 30 min. Slides were then rinsed 3 times with 400 mM Tris, pH 7.5 and stained with ethidium bromide (0.2 μg/ml) for 1 min. Comets were analyzed using the Optronics DEI 750E CE Digital Output (Optronics, Goleta, CA) mounted on an Olympus BX40 fluorescence microscope. Fluorescence intensities were measured from 100 randomly selected cells for each biological repeat using the Comet Assay Software Project (CASP, [32]) and the extent of DNA damage reported as % Tail DNA.

2.3. Caspase-3 activity

Lysates from 2×10^6 THP-1 cells were prepared and incubated in a cytobuffer as previously described [10,33]. DEVD-AFC (20 μM) was used to determine caspase-3 activity. Released AFC was measured using a Cytofluor 400 fluorometer (Filters: excitation 400 nm, emission 508 nm; Perspective Co., Framingham, MA).

2.4. Identification of histone phosphorylation by LC–MS

Histones were isolated from THP-1 cells as described [34]. Briefly, 10^7 cells were washed with 10 mM Tris–HCl pH 7.5 and resuspended in NP-40-lysis buffer (0.1% NP-40, 10 mM Naglycerophosphate, 5 mM Na-pyrophosphate, 50 mM NaF, 1 mM sodium orthovanadate, 1 mM DTT, 0.1 mM PMSF, 2 μg/ml each of chymostatin, pepstatin, antipain, and leupeptin). After centrifugation, the pellets were collected and washed with Tris–HCl buffer and extracted with 0.4 N sulfuric acid followed by overnight precipitation in 80% acetone. The resulting precipitate was collected, dried, and dissolved in 100 μl of 20% acetonitrile (ACN) and 0.05% trifluoroacetic acid (TFA) solution. Histone modifications were characterized by liquid chromatography–mass spectrometry (LC–MS). LC–MS was performed using reversed-phase HPLC (Waters model 2690, Milford, MA) coupled to a MicroMass Q-TOF mass spectrometer (Micromass, Wythenshawe, Manchester, UK). Histone mixtures were separated on a 1.0 mm×150 mm C18 column (Discovery Bio wide pore C18 column, 5 μM, 300 Å, Supelco, Bellefonte, PA). Mobile phase A contained ACN with 0.05% TFA. Mobile phase B contained 0.05% TFA in HPLC grade water. Starting with 20% B, the gradient increased linearly to 30% B in 2 min, from 30% B to 35% B in 8 min, from 35% B to 50% B in 20 min, from 50% B to 60% B in 5 min, from 60% B to 95% B in 1 min and stayed in 95% for 4 min at the flow rate of 25 μl/min. LC–MS data was deconvoluted using the Masslynx 4.0 software package (Micromass, Wythenshawe, Manchester, UK). Phosphorylation of histones is indicated by the presence of species with a mass shift of +80 Da compared to the original mass.

2.5. Western blots

Cell lysates were prepared using lysis buffer (20 mM Hepes pH 7.4, 150 mM NaCl, 1 mM EDTA, 1.5 mM $MgCl_2$, 0.2% Tween-20, 10 mM Na-glycerophosphate, 5 mM Na-pyrophosphate, 50 mM NaF, 1 mM orthovanadate, 1 mM DTT, 0.1 mM PMSF, 2 μg/ml each of chymostatin, pepstatin, antipain, and leupeptin) for 30 min on ice and sonicated using a Branson Sonifier 450 (output control 3, duty cycle 30, pulses 3, Brason Ultrasonics Corporation, Danbury, CT) and centrifuged at 14,000 × *g* for 10 min at 4 °C. Equal amounts of protein were separated by SDS-PAGE, transferred onto nitrocellulose membranes and immunoblotted with primary antibodies followed by horseradish peroxidase-conjugated secondary antibodies and visualized by enhanced chemiluminescence (Amersham, Arlington Heights, IL). Anti-phospho-histone γH2AX (S139, clone JBW301) and anti-β-tubulin (clone AA2) antibodies were purchased from Millipore (Billerica, MA). Anti-ATM (clone Ab-3) antibodies were obtained from EMD-Bioscience (Gibbstown, NJ). Anti-phospho ATM (S1981, p-ATM), anti-phospho ATR (S428, p-ATR), and anti-ATR antibodies were from Abcam (Cambridge, MA). Anti-PKCδ (clone C-20) antibodies were purchased from Santa Cruz Biotechnology (Santa Cruz, CA). Anti-phospho-p38 (Thr180/Tyr182, p-p38) and total anti-p38 antibodies were from Cell Signaling (Boston, MA).

2.6. Immunoprecipitations and in vitro kinase assays

Cell lysates, prepared using NP-40 lysis buffer (0.5% NP-40, 50 mM Tris, pH 7.4, 10 mM Na-glycerophosphate, 5 mM Napyrophosphate, 50 mM NaF, 1 mM orthovanadate, 1 mM DTT, 0.1 mM PMSF, 2 μg/ml each of chymostatin, pepstatin, antipain, and leupeptin) for 30

min on ice, were immunoprecipitated overnight at 4 °C with 200 ng anti-PKCδ (clone C-20) antibodies or isogenic IgG as control (Santa Cruz Biotech.), followed by 1 h incubation with protein A-agarose beads. Immunoprecipitates were rinsed three times with NP-40 lysis buffer and twice with kinase buffer (25 mM Hepes pH 7.4, 10 mM $MnCl_2$, 1 mM $MgCl_2$, 1 mM DTT, 0.1 mM PMSF) and subjected to *in vitro* kinase assays for 1 h at 37 °C in the presence of 20 μl kinase buffer containing 2.5 μCi of [γ–^{32}P] ATP (PerkinElmer, Boston, MA), 0.5 μM ATP, 200 μg/ml phosphatidyl-serine, 20 μg/ml diacylglycerol and 2.5 μg of histone 2B (H2B, Boehringer Mannheim, Roche, Indianapolis, IN) as exogenous substrate. Reactions were stopped by the addition of 10 μl 5× Laemmli buffer, boiled, resolved by SDS-PAGE and subsequently transferred to membranes. Phosphorylated H2B was visualized by autoradiography and the same membranes were re-blotted with anti-PKCδ antibodies.

2.7. Immunofluorescence and cell cycle analysis

Cells were fixed with 2% paraformaldehyde for 10 min at room temperature (RT), rinsed twice with PBS, collected in slides by cytospinning centrifugation and subsequently permeabilized in 0.2% Triton X-100 at 4 °C for 15 min and blocked with PBS containing 1% FBS and 100 μg/ml human total IgG for 30 min at RT (Jackson ImmunoResearch Labs, Inc. West Grove, PA). Slides were incubated with 350 μg/ml anti-γH2AX antibodies for 1 h at RT, rinsed with PBS twice and incubated with 350 μg/ml anti-mouse antibodies Alexa Fluor 488 conjugated (Molecular Probes, Carlsbad, CA) for 1 h at RT. Slides were then rinsed twice with PBS and stained 5 min with 0.05 μg/ml DAPI at RT, washed twice with PBS and visualized using the Optronics DEI 750E CE Digital output mounted on Olympus BX40 fluorescence microscope.

For cell cycle analysis, THP-1 cells were washed with PBS prior to fixation in 70% ethanol, washed again with PBS twice and stained with propidium iodide (50 μg/ml; Sigma) containing 0.2 mg/ml DNAse-free RNAse (Roche, Indianapolis, IN) for 30 min at RT and immediately analyzed by FACS using the BD Cell Quest Pro software (BD biosciences, San Jose, CA).

2.8. siRNA silencing

Ten million THP-1 cells were transfected with 100 nM siRNA-p38 (Cell Signaling, Cat: 6386), siRNA scramble control (Qiagen, Valencia, CA; Cat: 1027284), or siRNA-PKCδ (Qiagen, Cat: 1027283) using the Amaxa nucleofector program V-001 (Lonza, Basel, Switzerland) as previously described [13]. Forty-hours after transfection, cells were treated with 50 μM apigenin or diluent DMSO for 3 h and analyzed.

2.9. Intracellular measurement of reactive oxygen species (ROS)

One million THP-1 cells were pre-treated with 20 μM EUK-134 for 1 h, prior to the addition of 50 μM apigenin for 1 h. Cells were rinsed with PBS twice and incubated in RPMI-1640 (without phenol red) in the presence of 10 μM DHE, a specific superoxide anion (O_2^-) probe, or 20 μM DCFDA, a general ROS probe, for 30 min at 37 °C, rinsed with PBS twice and visualized using the fluorescence microscope (Olympus BX40 equipped with the Optronics DEI 750E CE Digital Camera). Fluorescence intensities were measured from 50

randomly selected cells using the ImageJ software (National Institute of Health, Bathesda, MD).

2.10. Microarray analysis

Total RNA was isolated from THP-1 cells treated for 3 h with diluent DMSO or 50 μM apigenin using the RNEAsy mini Kit (Qiagen) following manufacture's instructions. RNA integrity was analyzed with the Agilent 2100 Bioanalyzer (Agilent Technology, Santa Clara, CA). cDNA was synthesized and used to hybridize a Human Gene 1.0 ST Array Data Set chips (Affimetryx, Santa Clara, CA) at the Microarray Shared Resource (The Ohio State University-Comprehensive Cancer Center). The array analyzed 28,869 annotated human genes with 764,885 distinct probes. All experiments were performed in triplicates with independent pools of RNA from three biological repeats using six separate microarray chips. Signal intensities, background correction, and normalization were performed using the Affymetrix Expression Consol software and applying the RMA method (Affymetrix). Oneway ANOVA was applied to analyze the normalized data using the R 2.9.0 software. The variance shrinkage method was employed to improve the estimates of variability and statistical tests of differentially expressed genes [35]. Genes significantly changing ($p < 0.01$) between groups with a fold change greater than 1.2 were further analyzed using Ingenuity Pathways Analysis (IPA) software (Ingenuity Systems, Redwood City, CA). IPA identified the biological functions, based on the Gene Ontology, that were most significant to the data set.

2.11. Quantitative RT-PCR (qRT-PCR) analysis

RNA was reverse transcribed to cDNA using the ThermoScript RT-PCR system (Invitrogen) according to manufacture's instructions. A 20 μl mixture containing 2 μl of cDNA (20 ng) template, 0.25 μM primers and 10 μl SYBR Green Master Mix (Applied Biosystems, Carlsbad, CA) was run in an ABI 7900HT RT-PCR system using the Sequence Detection System (SDS) 2.2 software (Applied Biosystems) and the following conditions: 95 °C for 10 min, 40 cycles of 95 °C for 1 min, 60 °C for 1 min, and 72 °C for 1 min. Fold change in expression was calculated as: fold change = $2^{-\Delta Ct(Apigenin)}/2^{-\Delta Ct(DMSO)}$, where ΔCt = (Ct target − Ct reference). All selected genes were normalized to the expression of two internal controls: GAPDH and 18S. All primers used are described in Supplementary Table 1.

See Word document 1 as supplementary file. Supplementary material related to this article found, in the online version, at http://dx.doi.org/10.1016/j.bcp.2012.09.005.

2.12. Statistical analysis

All data are expressed as mean ± SEM and analyzed using GraphPad Prism (GraphPad Software, San Diego, CA). For cell cycle analysis, two-way ANOVA followed by Bonferroni's post hoc was used to assess statistical significance between means. For qRT-PCR results statistical significance was analyzed by the *t*-test. All other data was analyzed by one-way ANOVA followed by Bonferroni's post hoc comparisons. Statistical significance is stated in the text.

3. Results

3.1. Apigenin induces DNA damage

To better understand the early mechanisms associated with apigenin-induced cell death we examined whether apigenin affected DNA using the comet assay. THP-1 cells treated for 3 h with different concentrations of apigenin resulted in an increase dose–response relationship in the percentage of Tail DNA (% Tail DNA). The % Tail DNA increased from 10% and 20% in cells treated with 25 μM and 50 μM apigenin respectively, reaching almost 30% in cells treated with 100 μM apigenin (Fig. 1A, white arrows and B). Cells treated with the diluent DMSO (referred as control from now on) showed negligible levels of % Tail DNA and treatment with 1 mM H_2O_2 for 1 h, a known inducer of DNA-damage [36], showed approximately 50% Tail DNA, as previously reported (Fig. 1A and B) [36]. Next, we investigated the time-relationship of apigenin-induced DNA damage and the activation of caspase-3, a key apoptotic effector [10]. Cells treated for various times with 50 μM apigenin, a concentration previously reported as the IC_{50} for leukemia cells [10], showed a significant increased in % Tail DNA as early as 1 h after apigenin treatment, an increase that continued even after 9 h (Fig. 1C). Caspase-3 activity in these cells was barely detectable at 3 h after apigenin treatment, but significantly increased after 6 h (Fig. 1D). Collectively, these results indicate that apigenin induces DNA damage prior to the activation of caspase-3.

3.2. Apigenin induces H2AX phosphorylation

To gain insights into the mechanisms regulating apigenin-induced DNA damage, histone modifications were analyzed by LC–MS in THP-1 cells treated with 50 μM apigenin for 12 h. An increase in a molecular weight peak corresponding to phosphorylated H2AX was observed in apigenin-treated cells, compared with controls (Fig. 2A, red arrow, 15,133 Da peak referred as γH2AX). No other histone modifications were observed in apigenin-treated cells. The levels of non-phosphorylated H2AX were similar in apigenin-treated cells and control cells as indicated by the identical height of the 15,053 Da peak (Fig. 2A, black arrow). Levels of γH2AX increased ~2.5 fold at 1 h after apigenin treatment and continued augmenting reaching maximum levels at ~5 h (Fig. 2B) Formation of γH2AX nuclear foci, a characteristic of double strand breaks, was detected by immunofluorescence with γH2AX-specific antibodies in response to apigenin (Fig. 2C), at a time when DNA fragmentation, a hallmark of apoptosis, was not observed, as indicated by DAPI staining (Fig. 2C). Collectively, these results demonstrate that apigenin induces histone modifications characteristic of DNA damage, preceding the activation of the apoptotic program.

3.3. Apigenin-induced DNA damage is ROS and caspase 3-independent

We previously showed that apigenin induces ROS production as well as the activities of caspase-3, p38 and PKCδ [10,13]. To investigate the molecular mechanisms involved in apigenin-induced DNA damage, we examined the % Tail DNA in THP-1 cells pretreated for 1 h with 20 μM EUK-134, 20 μM DEVD-FMK, 10 μM SB203580, or 15 μM rottlerin (ROS, caspase-3, p38 and PKCδ inhibitors, respectively), prior to the addition of 50 μM apigenin for 3 h. Inhibition of ROS or caspase-3 had no effect in the % Tail DNA observed in apigenin-treated cells (Fig. 3A; EUK and DEVD; $p > 0.4$ white vs. black bars). Because, treatment with EUK failed to inhibit apigenin-induced DNA damage, we investigated

whether apigenin was inducing ROS production using as an independent method fluorescent dies. In agreement with previous results using electron paramagnetic resonance [10], we observed that treatment with 50 μM apigenin induced ROS production significantly at 1 h, as demonstrated by an increase of ~4 folds in DCFDA fluorescence (Fig. 3B, black bars) and ~4 times increased in superoxide anion (O_2^-) levels using DHE fluorescence (Fig. 3B, white bars). To further investigate that the lack of inhibition of apigenin-DNA damage was not due to the failure of EUK to inhibit ROS production, we determined ROS levels in apigenin-treated cells pretreated with EUK. We found that EUK successfully inhibited apigenin-induced ROS (Fig. 3B). In contrast, the % Tail DNA was reduced by almost 50% in cells pretreated with the p38 inhibitor SB203580, while inhibition of PKCδ decreased the % Tail DNA to levels found in controls (Fig. 3A). Taken together, these findings indicate that, while apigenin is capable of inducing ROS and caspase-3 activity, they are not required for DNA damage.

3.4. PKCδ and p38 are required for apigenin-induced DNA damage

To investigate the mechanisms involved in apigenin-induced DNA damage we evaluated the signaling network mediating γH2AX. Pretreatment with the PKCδ inhibitor rottlerin (15 μM) for 1 h prior the addition of apigenin completely abrogated apigenin-induced γH2AX (Fig. 3C, compare lanes 8–10 and lanes 2–4), whereas inhibition of p38 with 10 μM SB203580 significantly reduced γH2AX (Fig. 3C, compare lanes 5–7 and lanes 2–4). In addition, inhibition of PKCδ resulted in a slight increase of p38 phosphorylation in apigenin-treated cells (Fig. 3C, compare lanes 8–10 and lanes 2–4), whereas inhibition of p38 reduced PKCδ activity to levels found in controls, as indicated by the reduced phosphorylation of H2B in *in vitro* kinase assays (Fig. 3D, compare lanes 4 vs. 3).

Next, we evaluated the effect of apigenin on ATM and ATR phosphorylation, key γH2AX regulators. ATM phosphorylation increased rapidly 30 min after the treatment with 50 μM apigenin and the phosphorylation remained high even after 6 h, compared with control cells (Fig. 4A). In contrast, no change in ATR phosphorylation was observed in cells treated with apigenin (Fig. 4A). To investigate the role of PKCδ and p38 on apigenin-induced ATM phosphorylation, cells were pretreated with 15 μM rottlerin or 10 μM SB203580 for 1 h prior the addition of 50 μM apigenin. Inhibition of PKCδ resulted in a reduction of ATM phosphorylation to levels observed in control cells (Fig. 4B, compare lanes 8–10 and lanes 2–4). In contrast, inhibition of p38 had no effect on apigenin-induced ATM phosphorylation (Fig. 4B, compare lanes 5–7 and lanes 2–4). To further define the signaling network, PKCδ or p38 were silenced with siRNA-PKCδ or siRNA-p38 respectively, and phosphorylation of H2AX and ATM were evaluated in cells treated with 50 μM apigenin or diluent control for 3 h. Silencing of PKCδ decreased apigenin-induced γH2AX and ATM phosphorylation to levels found in siRNA-control cells, but had no effect on apigenin-induced p38 phosphorylation (Fig. 4C, compare lane 6 and lane 2). However, silencing of p38 reduced apigenin-induced γH2AX, but had no effect on apigenin-induced ATM phosphorylation (Fig. 4C, compare lane 4 and lane 2). Taken together, these results indicate a complex crosstalk between p38 and PKCδ, both capable of regulating γH2AX during apigenin-induced DNA damage and suggest a central role of PKCδ in the phosphorylation of ATM.

3.5. Apigenin affects cell cycle progression and gene expression

To investigate the molecular mechanisms involved in apigenin-dependent responses to DNA damage, we examined cell cycle profiles of THP-1 cells treated with control or with increasing concentrations of apigenin for 24 h and monitored the DNA content by PI staining. A significant decrease of cells with 4N content, from ~25% found in control cells to 10% in cells treated with 50 μM apigenin was observed (Fig. 5A and B). This effect was accompanied by a significant accumulation of Sub-G1 cells from 5% in control cells to ~15 and 20% in cells treated with 25 and 50 μM apigenin, respectively (Fig. 5A and B) and an increase of cells with 2N content from 40% in control cells to 50% in cells treated with 25 or 50 μM apigenin, indicative of a G1 arrest (Fig. 5A and B). No significant differences were observed in cells treated with 10 μM apigenin and nocodazol, a treatment that induces G2/M arrest in leukemia cells [37]. These results indicate that apigenin induces G1 arrest in THP-1 cells while increasing the Sub-G1 cell population.

To investigate the effects of apigenin on gene expression genome wide, microarray analysis in THP-1 cells treated with 50 μM apigenin or diluent control for 3 h were performed. Of all the genes represented in the array, apigenin changed significantly the expression of ~8.5% (2390 genes), 81% of which were down-regulated (Supplementary Table 2). Functional categories analysis using Ingenuity Pathways Analysis (IPA) showed that the biological pathways most significantly affected by apigenin comprise gene expression, cell cycle, post-translation modification, DNA repair, and cell death (Fig. 5C). Consistent with the IPA analysis, heat map representation of the cell cycle genes showed that apigenin induced a significant change in 259 genes involved in the cell cycle, corresponding to ~10% of all cell cycle genes represented in the microarray (Fig. 5D). In addition, apigenin significantly changed 140 DNA repair genes, corresponding to ~5.5% of all DNA repair genes represented in the array (Fig. 5E).

See Excel sheet 1 as supplementary file. Supplementary material related to this article found, in the online version, at http://dx.doi.org/10.1016/j.bcp.2012.09.005.

In agreement with the microarray data, qRT-PCR showed that the expression of cell cycle genes including cyclin E1 (CCNE1), cyclin E2 (CCNE2), E2F2, Myc, and cdc25a was significantly decreased in cells treated with 50 μM apigenin for 3 h when compared to controls (Fig. 5F). Moreover, apigenin decreased the expression of DSBs repair genes such as BACH1, FEN1, XRCC2, POLH and RAD1 (Fig. 5F). Consistent with the microarray data, CDK2 expression was not affected, suggesting a specific set of G1/S genes being modulated by apigenin (Fig. 5F and Supplementary Table 2). All together, our results indicate that apigenin induces DNA damage leading to down-regulation of genes involved in cell cycle regulation and DNA repair while inducing cell death.

4. Discussion

Flavonoids are emerging as potent alternative anti-cancer agents. However, their mechanisms of action remain poorly defined. The present study demonstrates that apigenin-induced activation of the apoptotic pathway is preceded by p38 and PKCδ-dependent DNA damage and independent of ROS production. Apigenin induced PKCδ-dependent activation

of ATM and H2AX phosphorylation, whereas p38 regulated H2AX phosphorylation but had no effect in ATM, suggesting a complex regulatory network (Fig. 6). Consistently, apigenin triggered changes in gene expression characterized by the down-regulation of DNA repair and cell cycle transition genes. Taken together, the current study provides novel insights of the signaling networks and the molecular mechanisms involved in the cytotoxic effects of apigenin (Fig. 6).

Commonly used chemotherapeutic drugs, such as etoposide, camptothecin, and doxorubicin are topoisomerase poisons that trigger apoptosis by inducing DSBs leading to DNA damage [16–18]. Limited understanding on the molecular mechanisms responsible for the cytotoxic effects of flavonoids hampers their utilization. Flavonoids such as genistein, luteolin and apigenin, induce topoisomerase dependent DNA damage *in vitro* [38,39]. Previous studies showed that, in HL-60 leukemia cells apigenin induced DNA fragmentation, a result of the activation of caspase-3, a key regulator of apoptosis [40,41]. We found that while DNA damage increased over the experimental time, it was detected prior to the activation of caspase-3, noted only 3 h after apigenin treatment (Fig. 1C and D). Consistently, the caspase-3 inhibitor DEVD-FMK failed to block apigenin-induced DNA damage (Fig. 3A). Thus, it is possible that one of the mechanisms by which apigenin triggers apoptosis is by inducing DNA damage, which in turn results in the activation of the apoptotic cascade (Fig. 6).

DNA damage was accompanied by an increase of H2AX phosphorylation, an epigenetic change characteristic of DNA damage and foci formation (Fig. 2). γH2AX, a marker of DSBs has an important role in the DNA damage response and is modulated through a complex signaling network including ATM and ATR kinases [23–26]. We found that apigenin induced robust ATM phosphorylation at 30 min post-treatment, consistently with the kinetics of γH2AX, but no changes on ATR phosphorylation (Fig. 4A).

We previously reported that apigenin induces a transient production of ROS [10], prompting us to investigate whether apigenin-induced DNA damage was ROS related. Notably, we found that apigenin-induced DNA damage was ROS independent (Fig. 3A and B). Although ROS induces oxidative DNA damage and single strand beaks, these events might be rapidly repaired after removal of the free radicals. Moreover, we previously reported that apigenin-induced caspase-3 activation was ROS independent [10], further supporting the hypothesis that the generation of ROS is not involved directly in the cytotoxic effects of apigenin. The flavone luteolin was shown to induce DNA damage and apoptosis by affecting topoisomerase II activity in human promyelocytic leukemia cells [42]. Consistent with our results, luteolin-induced DNA damage was ROS independent [42]. In contrast, quercetin induced ROS-dependent DNA damage [42], being found to exert its DNA damaging effects via metal-catalyzed oxidation with the subsequent generation of ROS [43–45]. Thus, while flavonols induce DNA damage via production of ROS, flavones such as apigenin may exert its clastogenic effect by inhibiting topoisomerases, further aggravated by the activation of PKCδ.

To further elucidate the mechanisms of apigenin-induced DNA damage we looked at the role of PKCδ and MAPK kinases. PKCδ and p38 are activated in response to multiple

genotoxic agents and have been shown to regulate DNA-damage response pathways [28,29,46–48]. We previously reported that apigenin induces ERK activation after 3 h of apigenin treatment, suggesting that ERK is not involved in the early apigenin-induced DNA damage [10,13]. In contrast, p38 and PKCδ activity arose with similar kinetics as apigenin-induced DNA damage. Herein, we found that pharmacological inhibition and silencing of PKCδ completely abolished apigenin-induced DNA strand breaks, γH2AX and p-ATM, indicating that these events are dependent on the activity of PKCδ (Figs. 3 and 4). In contrast, inhibition of p38 only partially attenuated apigenin-induced DNA strand breaks and γH2AX but had not effect on p-ATM, suggesting that PKCδ is the main player in promoting apigenin-induced DSBs (Figs. 3 and 4). Pharmacological inhibition of p38 decreased stress-induced γH2AX in leukemia, keratinocyte and myeloma cells [47–50]. Consistent with our results, it has been shown that p38 phosphorylates H2AX *in vitro* [47] and regulates DNA-damage response downstream of ATM in response to doxorubicin and cisplatin in p53-deficient cells [51]. On the other hand, pharmacological inhibition of PKCδ abrogated etoposide-induced DNA fragmentation, γH2AX and ATM phosphorylation in acinar and epithelial cells [28,29], indicating the relevance of PKCδ in DNA damage. Although several models have been suggested, the mechanisms on how PKCδ regulates the DNA damage response remain elusive [29,46,52,53]. Therefore, a mechanism can be proposed in which apigenin-induced PKCδ activity inhibits endogenous DNA repair while promoting DNA strand breaks and apoptosis. Further experiments will be necessary to address this possibility.

In response to DSBs, ATM phosphorylates many cell cycle checkpoint-related factors such as γH2AX, p53, and Chk1 leading to cell cycle arrest, and eventually apoptosis [54]. We found that apigenin decreased the G2/M population, followed by an increased of cells in G1 and Sub-G1 (Fig. 5B). It has been previously noted that apigenin affects the cell cycle [11,55–59]. Exposure of a wide array of malignant cells to apigenin induced G2/M or G1/G0 arrest regardless of their Rb and p53 status, indicating that the modulation of cell cycle by apigenin is p53 independent [11,55–59]. Our results further support these findings due to the p53-deficient status of THP-1 cells [60]. The reasons for these differences are yet to be uncovered but may reflect the existence of cell type specific signaling cascades.

To determine the mechanisms responsible for apigenin-induced cell cycle arrest and apoptosis we performed genome wide mRNA expression analysis. Apigenin significantly down-regulated genes involved in cell cycle control and DNA repair. These observations were confirmed by qRT-PCR and were consistent with the induction of DNA damage and cell cycle arrest by apigenin. Microarray analysis was previously performed in prostate cancer cells treated with luteolin [61]. Consistent with our findings, among the biological pathways most significantly affected by that flavone were gene expression, cell cycle, cell death and DNA repair [61]. Interestingly, the expression of ~80% of the genes affected by luteolin were also down-regulated. We observed more than 500 genes that were commonly changed in both studies constituting potential transcriptional targets of flavones. Cyclin E1, cyclin E2, cdc25a, E2Fs, and myc, among others, were down-regulated in both arrays. E2F2 and myc are transcription factors that regulate the expression of genes involved in cell cycle progression such as cyclins E1 and E2 [62]. Cyclins E1 and E2 bind to cyclin dependent

kinase 2 (CDK2) promoting its activity and the cell cycle transition from G1 to S [63]. Apigenin decreased the expression of genes involved in the DNA damage response including BACH1, XRCC2, DNA polymerase η (POLH), and RAD1. Besides the genes confirmed by qRT-PCR, other molecules involved in cell cycle control and DNA repair were strongly affected by apigenin in the array, such as GADD45A (growth arrest and DNA-damage-inducible, alpha), GADD45B, GSPT2 (G1 to S transition protein 2), CDC6 (Cell cycle division 6), WEE1, MSH6 (mutS homolog 6), FEN1 (flap structure-specific endonuclease 1), EXO1 (exonuclease 1), and RFC1 (replication factor C 1), among other components of the basal transcriptional machinery (Supplementary Table 2). In addition, apigenin down-regulated the expression of POLR2D (RNA polymerase II polypeptide D), GTF2H4 (General transcription factor II H4), GTF2E1, GTF2B, and TBP (TATA box binding protein), among others (Supplementary Table 2). The effect of apigenin on general transcriptional mechanisms may explain the overall down-regulation of genes affected by apigenin. In conclusion, apigenin induces DNA damage through ATM activation and H2AX phosphorylation but independent of ATR. Activation of ATM and H2AX was PKCδ and p38 dependent leading to transcriptional down-regulation of genes involved in cell-cycle control and DSBs repair indicating that cells may be unable to repair apigenin-induced DNA damage, hence triggering apoptosis.

Supplementary Material

Refer to Web version on PubMed Central for supplementary material.

Acknowledgments

The authors acknowledge financial support from the Ohio Plant Biotechnology Consortium (OPBC) to AID and the PHPID-Program fellowship to D.A. We thank Dr. Xiaokui Mo (Center for Biostatistics, The Ohio State University) for help with the bioinformatic analysis of microarray data.

References

[1]. Ross JA, Kasum CM. Dietary flavonoids: bioavailability, metabolic effects, and safety. Annu Rev Nutr. 2002; 22:19–34. [PubMed: 12055336]

[2]. Middleton E Jr, Kandaswami C, Theoharides TC. The effects of plant flavonoids on mammalian cells: implications for inflammation, heart disease, and cancer. Pharmacol Rev. 2000; 52:673–751. [PubMed: 11121513]

[3]. Rice-Evans C, Spencer JP, Schroeter H, Rechner AR. Bioavailability of flavonoids and potential bioactive forms *in vivo*. Drug Metab Drug Interact. 2000; 17:291–310.

[4]. Havsteen BH. The biochemistry and medical significance of the flavonoids. Pharmacol Ther. 2002; 96:67–202. [PubMed: 12453566]

[5]. Nielsen SE, Young JF, Daneshvar B, Lauridsen ST, Knuthsen P, Sandstrom B, et al. Effect of parsley (*Petroselinum crispum*) intake on urinary apigenin excretion, blood antioxidant enzymes and biomarkers for oxidative stress in human subjects. Br J Nutr. 1999; 81:447–55. [PubMed: 10615220]

[6]. Yao Y, Sang W, Zhou M, Ren G. Phenolic composition and antioxidant activities of 11 celery cultivars. J Food Sci. 2010; 75:C9–13. [PubMed: 20492156]

[7]. Esposito K, Ciotola M, Giugliano F, De Sio M, Giugliano G, D'Armiento M, et al. Mediterranean diet improves erectile function in subjects with the metabolic syndrome. Int J Impot Res. 2006; 18:405–10. [PubMed: 16395320]

[8]. Skoldstam L, Hagfors L, Johansson G. An experimental study of a Mediterranean diet intervention for patients with rheumatoid arthritis. Ann Rheum Dis. 2003; 62:208–14. [PubMed: 12594104]

[9]. Gates MA, Vitonis AF, Tworoger SS, Rosner B, Titus-Ernstoff L, Hankinson SE, et al. Flavonoid intake and ovarian cancer risk in a population-based case-control study. Int J Cancer. 2009; 124:1918–25. [PubMed: 19117058]

[10]. Vargo MA, Voss OH, Poustka F, Cardounel AJ, Grotewold E, Doseff AI. Apigenin-induced-apoptosis is mediated by the activation of PKCδ and caspases in leukemia cells. Biochem Pharmacol. 2006; 72:681–92. [PubMed: 16844095]

[11]. Shukla S, Gupta S. Apigenin-induced cell cycle arrest is mediated by modulation of MAPK, PI3K-Akt, and loss of cyclin D1 associated retinoblastoma dephosphorylation in human prostate cancer cells. Cell Cycle. 2007; 6:1102–14. [PubMed: 17457054]

[12]. Yin F, Giuliano AE, Law RE, Van Herle AJ. Apigenin inhibits growth and induces G2/M arrest by modulating cyclin-CDK regulators and ERK MAP kinase activation in breast carcinoma cells. Anticancer Res. 2001; 21:413–20. [PubMed: 11299771]

[13]. Gonzalez-Mejia ME, Voss OH, Murnan EJ, Doseff AI. Apigenin-induced apoptosis of leukemia cells is mediated by a bimodal and differentially regulated residue-specific phosphorylation of heat-shock protein-27. Cell Death Dis. 2010; 1:e64. [PubMed: 21364669]

[14]. Van Dross R, Xue Y, Knudson A, Pelling JC. The chemopreventive bioflavonoid apigenin modulates signal transduction pathways in keratinocyte and colon carcinoma cell lines. J Nutr. 2003; 133:3800S–4S. [PubMed: 14608117]

[15]. Shukla S, Gupta S. Apigenin: a promising molecule for cancer prevention. Pharm Res. 2010; 27:962–78. [PubMed: 20306120]

[16]. Lord CJ, Ashworth A. The DNA damage response and cancer therapy. Nature. 2012; 481:287–94. [PubMed: 22258607]

[17]. Nitiss JL. Targeting DNA topoisomerase II in cancer chemotherapy. Nat Rev Cancer. 2009; 9:338–50. [PubMed: 19377506]

[18]. Pommier Y. Topoisomerase I inhibitors: camptothecins and beyond. Nat Rev Cancer. 2006; 6:789–802. [PubMed: 16990856]

[19]. Rogakou EP, Pilch DR, Orr AH, Ivanova VS, Bonner WM. DNA double-stranded breaks induce histone H2AX phosphorylation on serine 139. J Biol Chem. 1998; 273:5858–68. [PubMed: 9488723]

[20]. Helt CE, Cliby WA, Keng PC, Bambara RA, O'Reilly MA. Ataxia telangiectasia mutated (ATM) and ATM and Rad3-related protein exhibit selective target specificities in response to different forms of DNA damage. J Biol Chem. 2005; 280:1186–92. [PubMed: 15533933]

[21]. Bakkenist CJ, Kastan MB. DNA damage activates ATM through intermolecular autophosphorylation and dimer dissociation. Nature. 2003; 421:499–506. [PubMed: 12556884]

[22]. Kastan MB, Lim DS. The many substrates and functions of ATM. Nat Rev Mol Cell Biol. 2000; 1:179–86. [PubMed: 11252893]

[23]. Cimprich KA, Cortez D. ATR: an essential regulator of genome integrity. Nat Rev Mol Cell Biol. 2008; 9:616–27. [PubMed: 18594563]

[24]. Zhou BB, Elledge SJ. The DNA damage response: putting checkpoints in perspective. Nature. 2000; 408:433–9. [PubMed: 11100718]

[25]. Kinner A, Wu W, Staudt C, Iliakis G. Gamma-H2AX in recognition and signaling of DNA double-strand breaks in the context of chromatin. Nucleic Acids Res. 2008; 36:5678–94. [PubMed: 18772227]

[26]. Lavin MF, Birrell G, Chen P, Kozlov S, Scott S, Gueven N. ATM signaling and genomic stability in response to DNA damage. Mutat Res. 2005; 569:123–32. [PubMed: 15603757]

[27]. Brodie C, Blumberg PM. Regulation of cell apoptosis by protein kinase cδ. Apoptosis. 2003; 8:19–27. [PubMed: 12510148]

[28]. Reyland ME, Anderson SM, Matassa AA, Barzen KA, Quissell DO. Protein kinase Cδ is essential for etoposide-induced apoptosis in salivary gland acinar cells. J Biol Chem. 1999; 274:19115–23. [PubMed: 10383415]

[29]. Clavijo C, Chen JL, Kim KJ, Reyland ME, Ann DK. Protein kinase Cδ-dependent and -independent signaling in genotoxic response to treatment of desferroxamine, a hypoxia-mimetic agent. Am J Physiol Cell Physiol. 2007; 292:C2150–60. [PubMed: 17563398]

[30]. Bulavin DV, Saito S, Hollander MC, Sakaguchi K, Anderson CW, Appella E, et al. Phosphorylation of human p53 by p38 kinase coordinates N-terminal phosphorylation and apoptosis in response to UV radiation. EMBO J. 1999; 18:6845–54. [PubMed: 10581258]

[31]. Singh NP, McCoy MT, Tice RR, Schneider EL. A simple technique for quantitation of low levels of DNA damage in individual cells. Exp Cell Res. 1988; 175:184–91. [PubMed: 3345800]

[32]. Konca K, Lankoff A, Banasik A, Lisowska H, Kuszewski T, Gozdz S, et al. A cross-platform public domain PC image-analysis program for the comet assay. Mutat Res. 2003; 534:15–20. [PubMed: 12504751]

[33]. Doseff AI, Baker JH Jr, Bourgeois TA, Wewers MD. Interleukin-4-induced apoptosis entails caspase activation and suppression of extracellular signal-regulated kinase phosphorylation. Am J Respir Cell Mol Biol. 2003; 29:367–74. [PubMed: 12663328]

[34]. Ren C, Zhang L, Freitas MA, Ghoshal K, Parthun MR, Jacob ST. Peptide mass mapping of acetylated isoforms of histone H4 from mouse lymphosarcoma cells treated with histone deacetylase (HDACs) inhibitors. J Am Soc Mass Spectrom. 2005; 16:1641–53. [PubMed: 16099169]

[35]. Smyth GK. Linear models and empirical bayes methods for assessing differential expression in microarray experiments. Stat Appl Genet Mol Biol. 2004; 3 Article3.

[36]. Visvardis EE, Tassiou AM, Piperakis SM. Study of DNA damage induction and repair capacity of fresh and cryopreserved lymphocytes exposed to H_2O_2 and γ-irradiation with the alkaline comet assay. Mutat Res. 1997; 383:71–80. [PubMed: 9042421]

[37]. Matkovic K, Lukinovic-Skudar V, Banfic H, Visnjic D. The activity of extracellular signal-regulated kinase is required during G2/M phase before metaphase-anaphase transition in synchronized leukemia cell lines. Int J Hematol. 2009; 89:159–66. [PubMed: 19148588]

[38]. Boege F, Straub T, Kehr A, Boesenberg C, Christiansen K, Andersen A, et al. Selected novel flavones inhibit the DNA binding or the DNA religation step of eukaryotic topoisomerase I. J Biol Chem. 1996; 271:2262–70. [PubMed: 8567688]

[39]. Bandele OJ, Osheroff N. Bioflavonoids as poisons of human topoisomerase II alpha and II beta. Biochemistry. 2007; 46:6097–108. [PubMed: 17458941]

[40]. Wang IK, Lin-Shiau SY, Lin JK. Induction of apoptosis by apigenin and related flavonoids through cytochrome c release and activation of caspase-9 and caspase-3 in leukaemia HL-60 cells. Eur J Cancer. 1999; 35:1517–25. [PubMed: 10673981]

[41]. Janicke RU, Sprengart ML, Wati MR, Porter AG. Caspase-3 is required for DNA fragmentation and morphological changes associated with apoptosis. J Biol Chem. 1998; 273:9357–60. [PubMed: 9545256]

[42]. Yamashita N, Kawanishi S. Distinct mechanisms of DNA damage in apoptosis induced by quercetin and luteolin. Free Radic Res. 2000; 33:623–33. [PubMed: 11200093]

[43]. Liu Y, Deng K, Li J, Liu S, Yao S. Investigation of double stranded DNA damage induced by quercetin-copper(II) using piezoelectric quartz crystal impedance technique and potentiometric stripping analysis. Biophys Chem. 2004; 112:69–76. [PubMed: 15501577]

[44]. Rahman A, Fazal F, Greensill J, Ainley K, Parish JH, Hadi SM. Strand scission in DNA induced by dietary flavonoids: role of Cu(I) and oxygen free radicals and biological consequences of scission. Mol Cell Biochem. 1992; 111:3–9. [PubMed: 1588940]

[45]. Fazal F, Rahman A, Greensill J, Ainley K, Hadi SM, Parish JH. Strand scission in DNA by quercetin and Cu(II): identification of free radical intermediates and biological consequences of scission. Carcinogenesis. 1990; 11:2005–8. [PubMed: 2171797]

[46]. Yoshida K, Yamaguchi T, Shinagawa H, Taira N, Nakayama KI, Miki Y. Protein kinase Cδ activates topoisomerase IIα to induce apoptotic cell death in response to DNA damage. Mol Cell Biol. 2006; 26:3414–31. [PubMed: 16611985]

[47]. Lu C, Shi Y, Wang Z, Song Z, Zhu M, Cai Q, et al. Serum starvation induces H2AX phosphorylation to regulate apoptosis via p38 MAPK pathway. FEBS Lett. 2008; 582:2703–8. [PubMed: 18619440]

[48]. Rakkestad KE, Skaar I, Ansteinsson VE, Solhaug A, Holme JA, Pestka JJ, et al. DNA damage and DNA damage responses in THP-1 monocytes after exposure to spores of either Stachybotrys chartarum or Aspergillus versicolor or to T-2 toxin. Toxicol Sci. 2010; 115:140–55. [PubMed: 20150440]

[49]. Kobayashi T, Kuroda J, Ashihara E, Oomizu S, Terui Y, Taniyama A, et al. Galectin-9 exhibits anti-myeloma activity through JNK and p38 MAP kinase pathways. Leukemia. 2010; 24:843–50. [PubMed: 20200560]

[50]. Hsiao PW, Chang CC, Liu HF, Tsai CM, Chiu TH, Chao JI. Activation of p38 mitogen-activated protein kinase by celecoxib oppositely regulates survivin and (H2AX in human colorectal cancer cells. Toxicol Appl Pharmacol. 2007; 222:97–104. [PubMed: 17540426]

[51]. Reinhardt HC, Aslanian AS, Lees JA, Yaffe MB. p53-Deficient cells rely on ATM-and ATR-mediated checkpoint signaling through the p38MAPK/MK2 pathway for survival after DNA damage. Cancer Cell. 2007; 11:175–89. [PubMed: 17292828]

[52]. Bharti A, Kraeft SK, Gounder M, Pandey P, Jin S, Yuan ZM, et al. Inactivation of DNA-dependent protein kinase by protein kinase Cδ: implications for apoptosis. Mol Cell Biol. 1998; 18:6719–28. [PubMed: 9774685]

[53]. Emoto Y, Manome Y, Meinhardt G, Kisaki H, Kharbanda S, Robertson M, et al. Proteolytic activation of protein kinase Cδ by an ICE-like protease in apoptotic cells. EMBO J. 1995; 14:6148–56. [PubMed: 8557034]

[54]. Matsuoka S, Ballif BA, Smogorzewska A, McDonald ER 3rd, Hurov KE, Luo J, et al. ATM and ATR substrate analysis reveals extensive protein networks responsive to DNA damage. Science. 2007; 316:1160–6. [PubMed: 17525332]

[55]. Zheng PW, Chiang LC, Lin CC. Apigenin induced apoptosis through p53-dependent pathway in human cervical carcinoma cells. Life Sci. 2005; 76:1367–79. [PubMed: 15670616]

[56]. Takagaki N, Sowa Y, Oki T, Nakanishi R, Yogosawa S, Sakai T. Apigenin induces cell cycle arrest and p21/WAF1 expression in a p53-independent pathway. Int J Oncol. 2005; 26:185–9. [PubMed: 15586239]

[57]. Lepley DM, Pelling JC. Induction of p21/WAF1 and G1 cell-cycle arrest by the chemopreventive agent apigenin. Mol Carcinog. 1997; 19:74–82. [PubMed: 9210954]

[58]. McVean M, Weinberg WC, Pelling JC. A p21(waf1)-independent pathway for inhibitory phosphorylation of cyclin-dependent kinase p34(cdc2) and concomitant G(2)/M arrest by the chemopreventive flavonoid apigenin. Mol Carcinog. 2002; 33:36–43. [PubMed: 11807956]

[59]. Lepley DM, Li B, Birt DF, Pelling JC. The chemopreventive flavonoid apigenin induces G2/M arrest in keratinocytes. Carcinogenesis. 1996; 17:2367–75. [PubMed: 8968050]

[60]. Shiohara M, Akashi M, Gombart AF, Yang R, Koeffler HP. Tumor necrosis factor alpha: posttranscriptional stabilization of WAF1 mRNA in p53-deficient human leukemic cells. J Cell Physiol. 1996; 166:568–76. [PubMed: 8600160]

[61]. Shoulars K, Rodriguez MA, Thompson T, Markaverich BM. Regulation of cell cycle and RNA transcription genes identified by microarray analysis of PC-3 human prostate cancer cells treated with luteolin. J Steroid Biochem Mol Biol. 2010; 118:41–50. [PubMed: 19837161]

[62]. Cobrinik D. Regulatory interactions among E2Fs and cell cycle control proteins. Curr Top Microbiol Immunol. 1996; 208:31–61. [PubMed: 8575212]

[63]. Malumbres M, Barbacid M. Cell cycle, CDKs and cancer: a changing paradigm. Nat Rev Cancer. 2009; 9:153–66. [PubMed: 19238148]

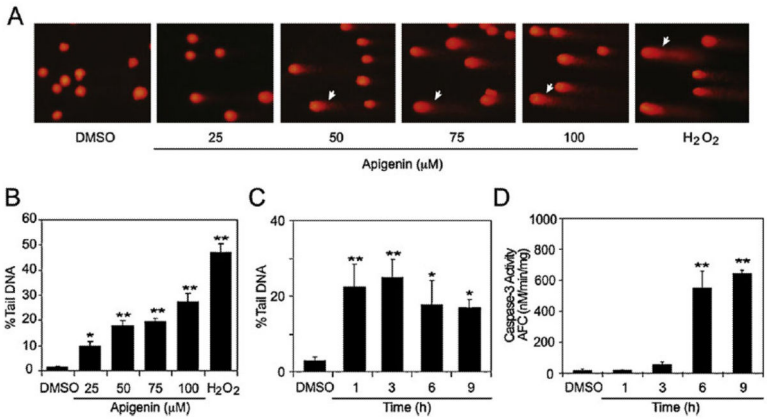

Fig. 1.

Apigenin induces DNA damage in leukemia cells. (A) Comet assays of THP-1 cells treated with indicated concentrations of apigenin or diluent DMSO for 3 h or with 1 mM H_2O_2 for 1 h. (B) % Tail DNA determined by alkaline comet assay in cells treated as described in (A). (C) % Tail DNA in cells treated with 50 μM apigenin for different lengths of time or diluent DMSO for 9 h. (D) Caspase-3 activity was determined in cells treated as described in (C). Data represents mean ± SEM, $n = 3$. *$p < 0.05$, **$p < 0.01$, compared to DMSO control.

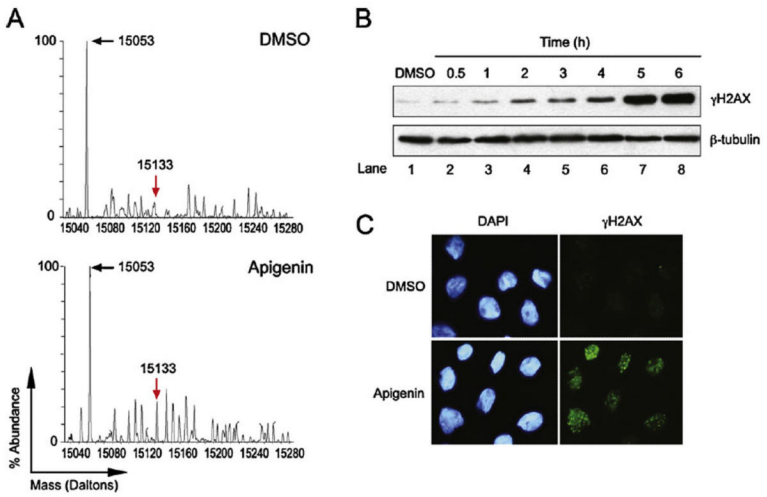

Fig. 2.

Apigenin induces H2AX phosphorylation. (A) Epigenetic changes were analyzed by LC–MS in THP-1 cells treated with DMSO or 50 μM apigenin for 12 h (upper and lower panel, respectively). Black and red arrows indicate peaks corresponding to non-phosphorylated and phosphorylated H2AX, respectively. (B) Lysates from THP-1 cells treated with 50 μM apigenin for different time periods or diluent DMSO for 6 h were immunoblotted with γH2AX antibodies, membrane were re-blotted with β-tubulin antibodies. (C) THP-1 cells were immunostained with anti-γH2AX antibodies and counterstained with DAPI 3 h after treatment with 50 μM apigenin or DMSO. All results shown are representative of three independent experiments. (For interpretation of the references to color in this figure legend, the reader is referred to the web version of the article.)

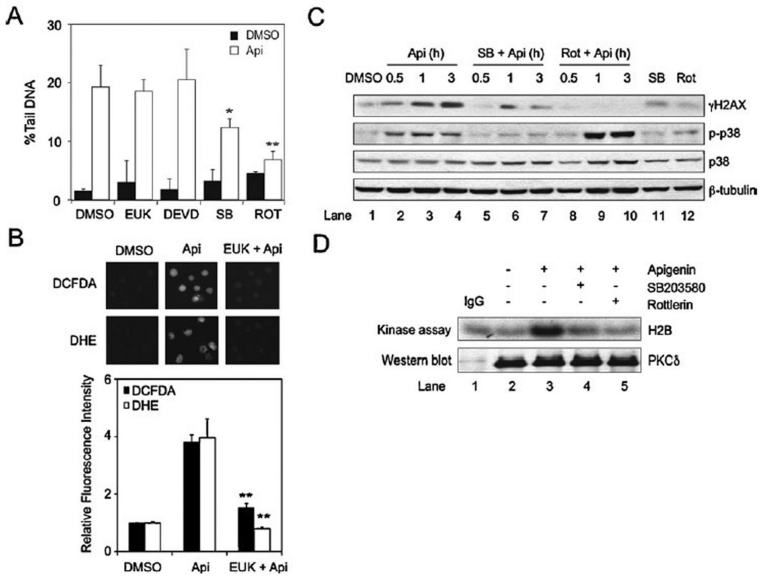

Fig. 3.

Apigenin-induced DNA damage is mediated by PKCδ and p38. (A) Comet assays of THP-1 cells pretreated for 1 h with 20 μM EUK-134, 20 μM DEVD-FMK, 10 μM SB203580 or 15 μM rottlerin prior to the addition of 50 μM apigenin or DMSO for 3 h (white and black bars respectively). Data represents the mean ± SEM, $n = 4$, $*p < 0.05$ and $**p < 0.01$ to apigenin treated cells. (B) THP-1 cells pre-treated with 20 μM EUK-134 for 1 h prior the addition of 50 μM apigenin or diluent DMSO for an additional hour were stained with DCFDA (black bars) or DHE (white bars) and visualized under the fluorescence microscope. Fluorescence intensity was determined using the ImageJ software. Data represents mean ± SEM, $n = 3$. $**p < 0.01$ compare EUK + Api and Api. (C) Lysates from THP-1 cells pretreated for 1 h with 10 μM SB203580, 15 μM rottlerin or DMSO prior the addition of 50 μM apigenin or diluent DMSO for the times indicated were immunoblotted with γH2AX, p-p38, p38 and β-tubulin antibodies. (D) Lysates from THP-1 cells treated with 50 μM apigenin in the presence or absence of 10 μM SB203580, 15 μM rottlerin or DMSO (indicated as –) were immunoprecipitated with anti-PKCδ antibodies or isogenic IgG control and subsequently subjected to *in vitro* kinase assays, phosphorylated H2B was visualized by autoradiography. The same membrane was immunoblotted with anti-PKCδ antibodies. Results are representative of three independent experiments.

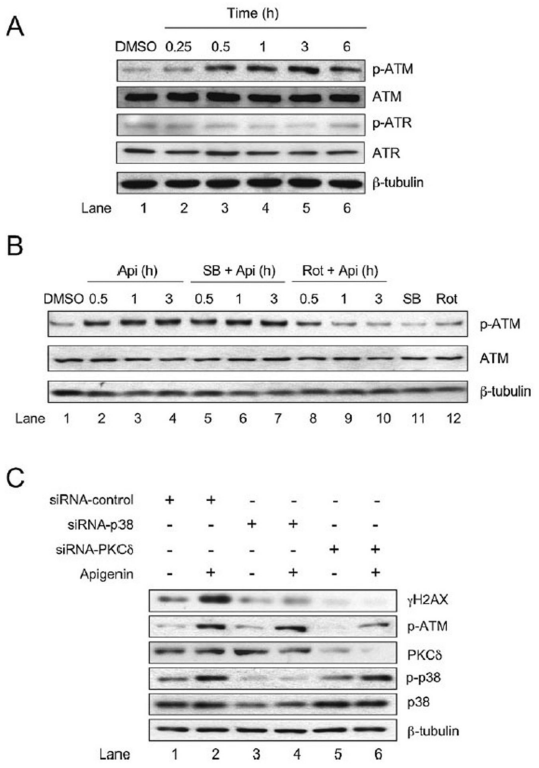

Fig. 4.

Apigenin induces ATM and γH2AX phosphorylation in a PKCδ and p38-dependent pathway. (A) Lysates of THP-1 cells treated with 50 μM apigenin for the indicated times or diluent DMSO for 6 h were immunoblotted with anti-phospho-ATM (p-ATM), anti-ATM, anti-phospho-ATR (p-ATR) and anti-ATR antibodies. (B) THP-1 cells were pretreated for 1 h with 10 μM SB203580 or 15 μM rottlerin prior to the addition of 50 μM apigenin for different time periods or diluent DMSO for 3 h. ATM phosphorylation was analyzed by western blot. (C) Lysates from THP-1 cells transfected with siRNA-control, siRNA-p38 or siRNA-PKCδ and subsequently treated with 50 μM apigenin or diluent DMSO for 3 h were analyzed by western blots with anti-γH2AX, p-ATM, PKCδ, p-p38 or p38 antibodies. In all panels, the same membranes were re-blotted with anti-β-tubulin antibodies to ensure equal loading.

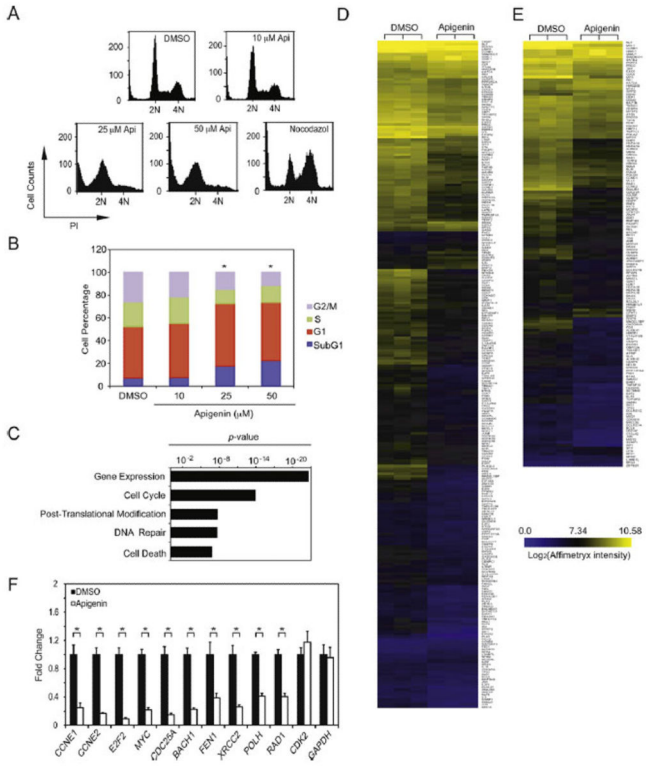

Fig. 5.

Apigenin affects cell cycle progression of THP-1 cells by transcriptionally repressing cell cycle and DNA repair genes. (A) Cell cycle distribution was analyzed in THP-1 cells treated for 24 h with various doses of apigenin, DMSO or 200 ng/ml nocodazol for 24 h. All results shown are representative of three independent experiments. (B) Percentage of cells in different stages of the cell cycle as indicated in (A). Data represents the mean ± SEM, $n = 3$, $^*p < 0.05$ compared to DMSO control as determined by two-way ANOVA followed by Bonferroni's post hoc. (C) Gene expression analysis of THP-1 cells treated with 50 μM apigenin or diluent control for 3 h. Genes significantly changing between groups ($p < 0.01$) with a fold change greater than 1.2 were analyzed using IPA according to the Gene Ontology Function. Bars correspond to functional categories significantly enriched in the data sets. (D) Heat map representation of cell cycle genes significantly modulated by apigenin (259 genes corresponding to 10.4% of total cell cycle genes). (E) Heat map representation of DNA repair genes significantly modulated by apigenin (140 genes corresponding to 5.5% of total DNA repair genes). (F) mRNA expression of selected genes was analyzed by qRT-PCR. Data represents the mean ± SEM. $n = 4$, $^*p < 0.05$.

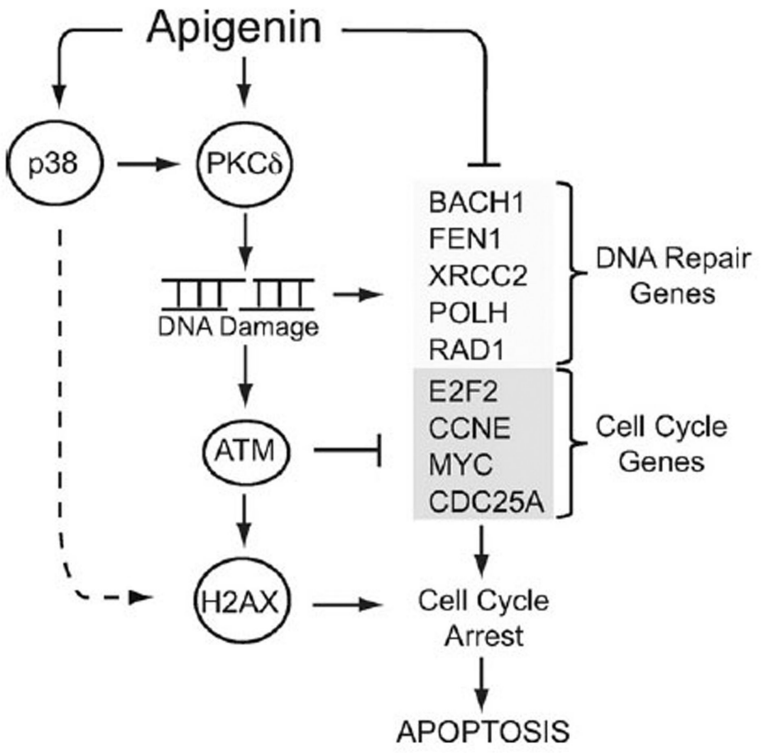

Fig. 6.

Working model of apigenin-induced DNA damage. Apigenin induces DSBs, ATM and H2AX phosphorylation in a PKCδ-dependent pathway, while p38 modulates apigenin-induced DNA damage independent of ATM. Apigenin-induced down-regulation of cell cycle control genes and ATM activation led to cell cycle arrest at the G1/S transition. Down-modulation of genes involved in DNA repair by apigenin indicates that cells may be unable to repair apigenin-induced DNA damage, hence triggering apoptosis.